CONF-900632--2

DE91 004408

ION-CHANNELING STUDY OF ANOMALOUS ATOMIC DISPLACEMENTS AT THE SUPERCONDUCTING TRANSITION IN HIGH-T_c MATERIALS*

L. E. REHN, R. P. SHARMA and P. M. BALDO

Materials Science Division
Argonne National Lab
Argonne, IL 60439, USA

June 1990

INVITED TALK to be presented at the C-MRS International'90 Conference, June 18-22, 1990, Beijing, China.

*Work supported by the U. S. Department of Energy, BES-Materials Sciences, under Contract W-31-109-Eng-38.

ION-CHANNELING STUDY OF ANOMALOUS ATOMIC DISPLACEMENTS AT THE SUPERCONDUCTING TRANSITION IN HIGH-T_c MATERIALS*

L. E. REHN, R. P. SHARMA and P. M. BALDO

Materials Science Division, Argonne National Lab, Argonne, IL 60439, USA

Ion channeling along the [001] direction in high-quality single crystals of (Y/Er)$Ba_2Cu_3O_{7-x}$ revealed an abrupt change in displacements in the a-b plane of the Cu and O atoms at the superconducting transition, T_c; normal "Debye-like" vibrations were found for the Y/Er and Ba atoms. The anomalous change in Cu-O displacements was found to shift directly with stoichiometry-induced changes in T_c, implying a direct link between the observed phonon anomaly and the superconducting transition. Recent measurements of ion-channeling along the [001] axis in $(Bi_{1.7}Pb_{0.3})Sr_2Ca_1Cu_2O_x$ single-crystals revealed a similar change at T_c, suggesting that this phonon anomaly is a general feature of high-T_c superconductivity.

In order to identify more specifically the crystallographic directions and displacement amplitudes associated with the anomalous phonon behavior, axial channeling scans using RBS, as well as characteristic x-ray production, were taken at several temperatures between 30 and 300K along the [301] and [331] directions of $YBa_2Cu_3O_{7-x}$ single crystals. Twins present in the specimens, and the existing static atomic displacements present along these directions, caused the channeling to be poorer along these axes compared to the (001) direction. Also, a much stronger dependence of the minimum yield on depth was observed. However, since only one twin variant generally dominated over sufficiently wide areas of the specimens, reasonably good (~10%) minimum yields could be obtained along the appropriate [331] axis, and detwinned crystals produced good results along [301].

1. INTRODUCTION

Several different experimental techniques, including neutron[1,2] and x-ray[3] diffraction, elastic constant measurements[4,5], and Raman scattering[6-8], have produced evidence of phonon anomalies at the superconducting transition in the class of high-T_c compounds represented by $RBa_2Cu_3O_{7-x}$ (where R denotes a rare earth element). The large amount of accumulated experimental evidence suggests that, as in conventional BCS superconductors, phonons play an important role in the high-T_c electron-pairing mechanism. Perhaps the clearest indication of anomalous phonon behavior in $RBa_2Cu_3O_{7-x}$ was provided by ion-channeling studies[9-11], in which an abrupt change at T_c in Cu-atom displacements perpendicular to the [001] axis was demonstrated.

We have recently[12] extended our ion-channeling investigations of phonon properties to $(Bi_{1.7}Pb_{.3})Sr_2Ca_1Cu_2O_x$, in search of a unifying explanation for high-T_c superconductivity. Although this material is structurally related (four-fold coordinated Cu-O layers) to the $RBa_2Cu_3O_{7-x}$ compounds, there are significant differences. For example, it is characterized by substantially less twinning, and it contains a strongly-modulated, incommensurate lattice structure[13,14]. Ion-channeling results obtained in single-crystals of $(Bi_{1.7}Pb_{.3})Sr_2Ca_1Cu_2O_x$ as a function of temperature between 35 and 295K revealed substantial effects on the channeling

* Work supported by the U. S. Department of Energy, BES-Materials Sciences, under Contract W-31-109-Eng-38.

behavior from the incommensurate lattice modulation that is known to exist in this material. In particular, the relatively large ($\lesssim$0.04 nm) static atomic displacements from this modulation[13,14] narrowed the critical angle for channeling by more than 50%, sharply reduced its expected temperature dependence, and increased the minimum yield by more than a factor of three. Of primary importance, however, these measurements[12] identified an anomaly across T_c in Cu-atom displacements perpendicular to the [001] axis that appears to be identical to the one found previously in $YBa_2Cu_3O_{7-x}$.

In this paper, we briefly review the ion-channeling evidence regarding the phonon anomaly at T_c in (Y/Er)$Ba_2Cu_3O_{7-x}$ and $(Bi_{1.7}Pb_{.3})Sr_2Ca_1Cu_2O_x$, focussing on a comparison of the ion-channeling characteristics in the two materials. We then present new data obtained from axial scans along the [301] and [331] axes in $YBa_2Cu_3O_{7-x}$.

2. ION CHANNELING ALONG [001] IN (Y/Er)$Ba_2Cu_3O_{7-x}$ AND $(Bi_{1.7}Pb_{.3})Sr_2Ca_1Cu_2O_x$

Ion-channeling[15] provides a direct, real-space probe of changes in atomic displacements as small as 1 pm. When an energetic ion beam is closely ($\lesssim$1°) aligned with a major crystallographic direction, the incident ions undergo a correlated sequence of small-angle collisions with the target atoms. As a result of these collisions, the ions are steered (channeled) between the atomic rows and planes of the lattice, causing a large reduction in small-impact-parameter events such as Rutherford backscattering (RBS) and innershell x-ray production. The critical angle of incidence for channeling to occur is determined by the ion energy, the atomic numbers of the projectile and target, the interatomic spacings, and any displacements (static plus thermal) of the atoms from their perfect lattice sites. Measurements of characteristic x-ray yields during channeling permit the displacements of the individual atomic species to be extracted more accurately than can be done using RBS alone. Most importantly, in contrast to the more traditional techniques used to determine phonon behavior, e.g. neutron and x-ray diffraction, inelastic neutron scattering, and elastic constant measurements, ion channeling is fully compatible with the small (~2 x 2 x 0.05 mm^3) and plate-like existing high-quality single crystals of the high-T_c materials.

Experimental details related to the present measurements can be found elsewhere.[9-12] Very briefly, single crystals of both materials were grown by a self-flux method.[16] Magnetic shielding measurements on the as-grown $(Bi_{1.7}Pb_{.3})Sr_2Ca_1Cu_2O_x$ samples showed sharp ($\lesssim$2K width) superconducting transitions centered at 90K. Annealing in flowing O produced similar transition characteristics (T_c = 92.8K; $\Delta T_c \lesssim$2K) in the (Y/Er)$Ba_2Cu_3O_{7-x}$ crystals. Samples were mounted with a metal-containing epoxy on a precision double-axis goniometer (angular resolution of 0.01°). The 0.5-mm-diameter analysis beam, 1.5- and 5.0-MeV ^4He for the RBS and x-ray measurements, respectively, was collimated to a divergence $\leq$0.05°. A solid-state RBS detector (FWHM = 16 keV; 30 mm^2 area) was positioned approximately 4 cm from the specimen at a scattering angle of 165°. A windowless liquid-nitrogen cooled Si(Li) x-ray detector, also 30 mm^2 in area, with an energy resolution of $\leq$200 eV at 8 keV, was mounted ~5 cm from the specimen at a scattering angle of 142°. Aluminum foil, approximately 25 μm thick, was used to shield the x-ray detector from the backscattered alpha particles. The vacuum in the chamber was $<5 \times 10^{-9}$ torr during analysis. The specimen temperature was monitored with a platinum resistance thermometer attached to the specimen stage, and could be stabilized to within ± 3° between 30 and 300K. Because of the sensitivity of these materials to irradiation damage,[9] the total dose on any one analyzed area was kept below 1×10^{15} ions/cm^2.

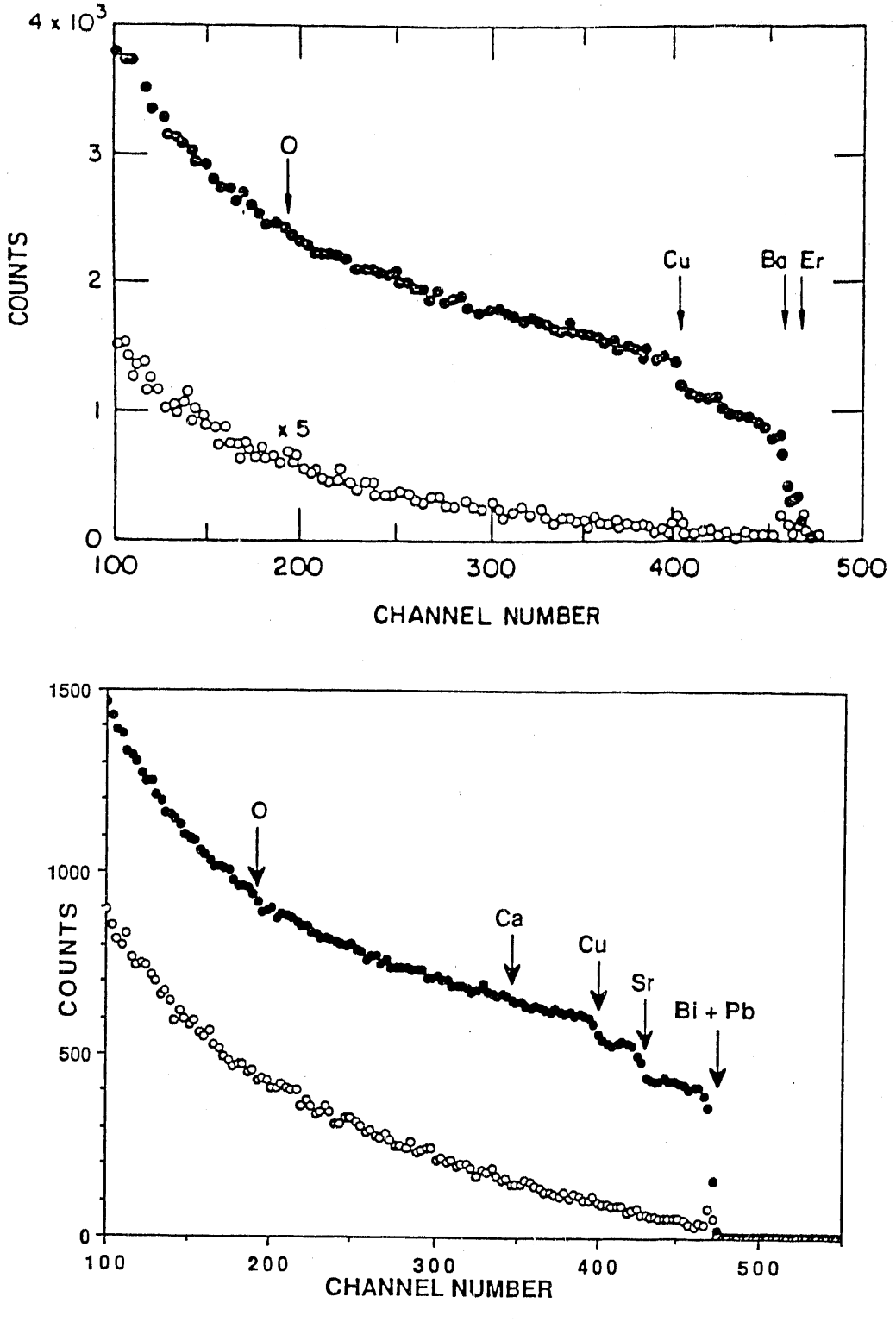

FIGURE 1
Aligned [001] and random RBS spectra from (a) $ErBa_2Cu_3O_{7-x}$ and (b) $(Bi_{1.7}Pb_{0.3})Sr_2Ca_1O_x$ single crystals.

An RBS spectrum from an $ErBa_2Cu_3O_{7-x}$ crystal taken at 80K with a 1.5 MeV ^4He beam incident along a random direction, and another with the same beam aligned along the [001] (c-axis) direction, are shown in Fig. 1a. Excellent channeling is observed. The aligned yield remains between 1.5% and 4% of the random yield over the entire analyzed depth (~1μm). The clearly separated Cu, Ba, and Er edges are denoted by the arrows at channel numbers 398, 452, and 461, respectively. The O edge is in channel number 193. Because the O signal magnitude is too low to yield statistically meaningful data at this He energy, no attempt was made to monitor that part of the spectrum during subsequent experiments. A similar pair of spectra taken from a $(Bi_{1.7}Pb_{.3})Sr_2Ca_1Cu_2O_x$ sample at 40K is shown in Fig. 1b. Again, the locations of the leading edges of the elemental constituents are indicated by arrows. Because of their similar masses, the Bi and Pb signals are indistinguishable. Reasonably good channeling is observed, but clearly not as good as for the $ErBa_2Cu_3O_{7-x}$ crystal. The aligned yield from the near-surface in the Bi and Pb portion of the spectrum (channels 430 to 475) is approximately 10% of the random count. By a depth (~700nm) corresponding to the O leading edge, the aligned yield has increased to >40% of the random. The near-surface minimum yield in Fig. 1b is, however, substantially improved over that obtained in the only known previous study of ion-channeling in single-crystals of this material. Kobayashi et al.[17] obtained minimum RBS yields >25% in $Bi_{2.2}Sr_{1.8}Ca_1Cu_2O_x$ even very close to the surface.

Examples of the channeling dips observed in the RBS yield from $ErBa_2Cu_3O_{7-x}$ as a function of specimen tilt angle about the [001] axis at temperatures above (100K) and below (80K) T_c are shown in Fig. 2a. The open circles represent RBS counts from only Er and Ba (channels 405-464; Fig. 1a), while the solid circles represent the combined RBS yield from Er, Ba and Cu (channels 225 to 384). The substantially greater width of the Er-Ba axial scans is a direct consequence of the high atomic numbers of Er and Ba; the lower minimum yield and more clearly defined compensating shoulders are due primarily to the higher energy range of the Er-Ba gate, which makes these measurements more surface sensitive. An increase of ~8% is seen in the FWHM of the combined Er-Ba-Cu axial scan as the temperature is lowered approximately 20 °K through T_c; essentially no change is seen in the FWHM of the Er-Ba scan over the same temperature interval.

Figs. 2b and 2c show [001] axial RBS scans taken at three different temperatures with a $(Bi_{1.7}Pb_{.3})Sr_2Ca_1Cu_2O_x$ sample. Those in (b) were acquired at 295, 100 and 60K with a gate (channels 409 to 464; Fig. 1b) set to accept only RBS counts from Bi, Pb and Sr, and those in (c) at temperatures of 295, 100 and 70K with a gate (channels 300 to 385) set to accept Bi, Pb, Sr and Cu counts. The somewhat (~10%) smaller FWHM in (c) is due primarily to the larger depth of analysis corresponding to this gate. The surface of this crystal was prepared by removing an ~50 μm thick layer from the as-grown surface using adhesive tape, resulting in an improved minimum yield ($\lesssim$7%) compared to Fig. 1b. The FWHM of the Bi-Pb-Sr gate increases from 1.03 to 1.06 to 1.07° as the temperature is lowered from 295 to 100 to 60K. The FWHM of the Bi-Pb-Sr-Cu scan increases from 0.89 to 0.94 to 0.99° over essentially the same temperature interval. Hence, in both superconductors, the scans containing the Cu RBS signal exhibit a significant (5-8%) change across T_c, while the other scan does not.

Axial scans similar to those shown in Fig. 2, were taken at several different temperatures between 30 and 300K in both materials. The FWHM obtained from these measurements are plotted as a function of temperature for $ErBa_2Cu_3O_{7-x}$ in Fig. 3a, and for $(Bi_{1.7}Pb_{.3})Sr_2Ca_1Cu_2O_x$ in Fig. 3b. The total increase in the

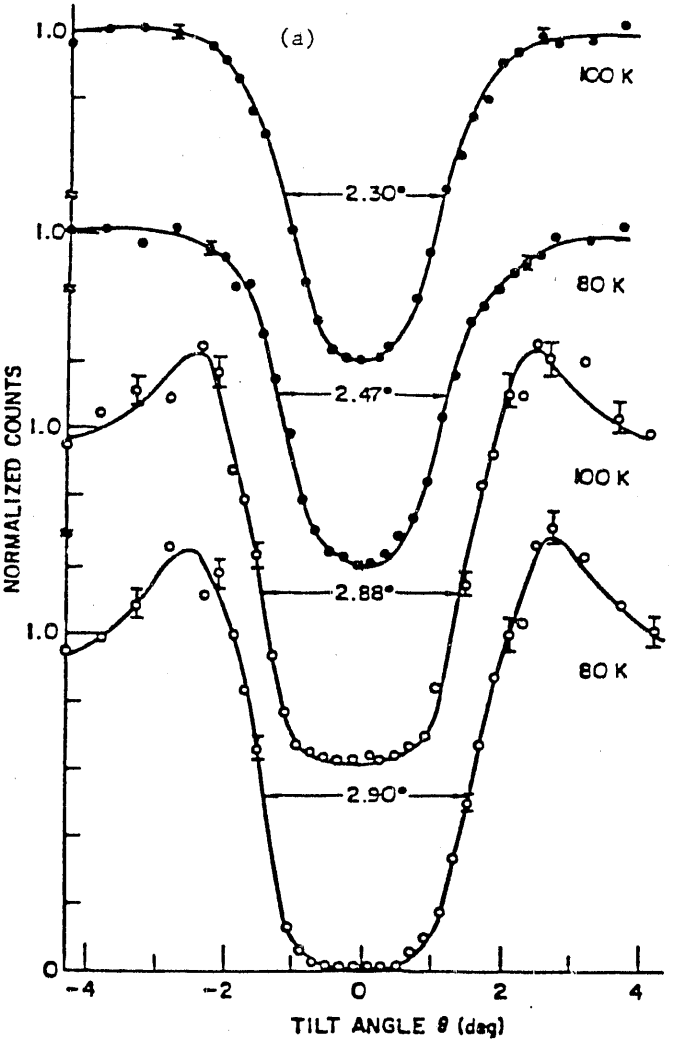

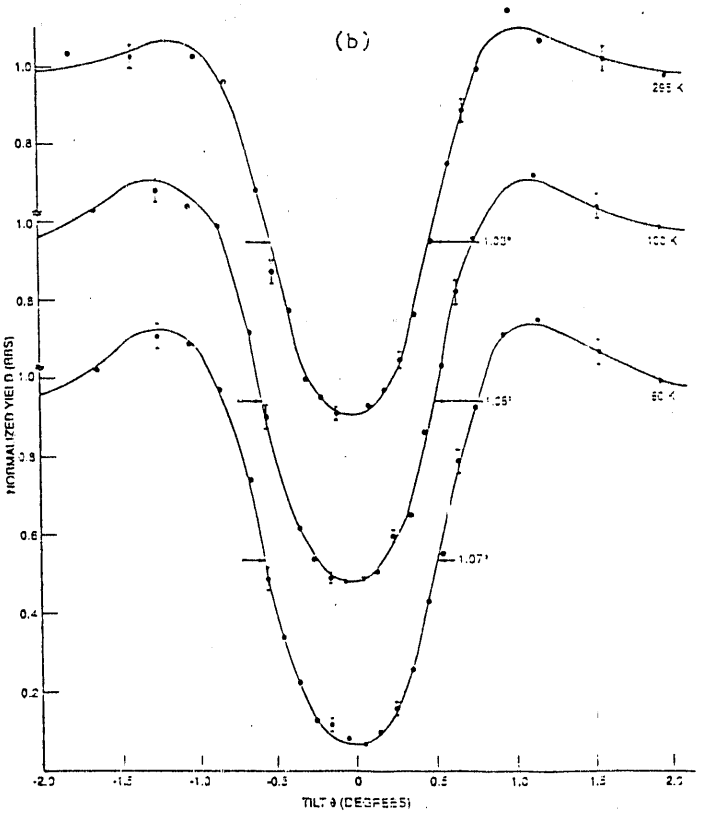

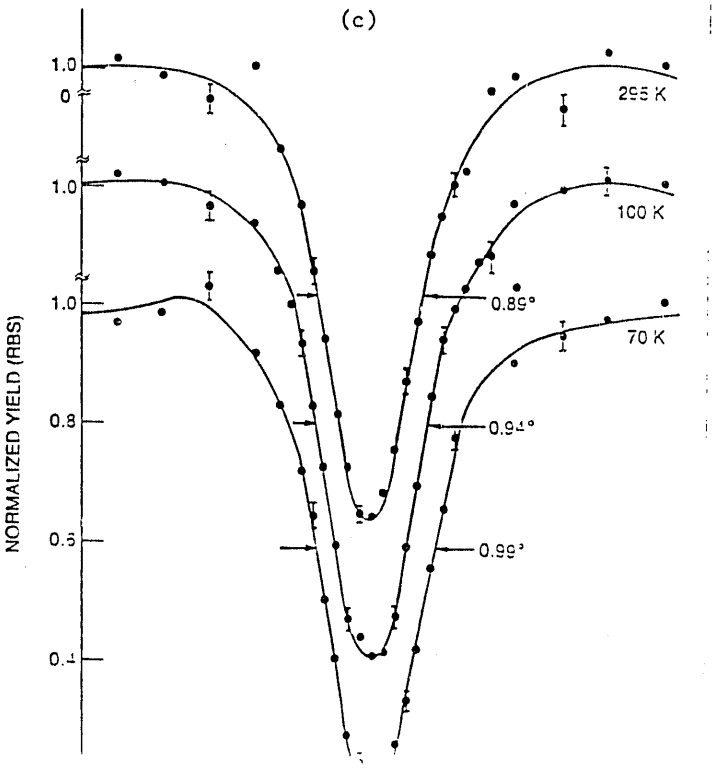

FIGURE 2
[001] axial scans above and below T_c for (a) an $ErBa_2Cu_3O_{7-x}$ single crystal (Er-Ba-Cu, solid circles; Er-Ba, open symbols) and for a $(Bi_{1.7}Pb_{0.3})Sr_2Ca_1Cu_2O_x$ single crystal: (b) Bi-Pb-Sr signal: (c) Bi-Pb-Cu signal.

FWHM of the scans from the $(Bi_{1.7}Pb_{.3})Sr_2Ca_1Cu_2O_x$ sample is considerably smaller than found for $ErBa_2Cu_3O_{7-x}$ between 295 and 60K. The net change is greater than 30% in (a), but $\lesssim$10% in (b). The high reproducibility of the $ErBa_2Cu_3O_{7-x}$ data can be seen in the sets of measurements taken just above (100K) and just below (80K) T_c; a standard deviation of <3% was determined for these data. A relatively smooth, monotonic decrease in the FWHM for the Er-Ba rows (open symbols; Fig. 3a) is seen with increasing temperature. We have shown previously[10] that this Er-Ba data can be fit very well to a Debye temperature dependence, with a characteristic temperature of 450 ± 25K. In contrast, the FWHM obtained using the Cu-Er-Ba data (solid circles; Fig. 3a) exhibit a significantly stronger temperature dependence, and an abrupt drop of ~7% in the FWHM is found between 80 and 100K. The anomalous drop is only slightly smaller than the 8% found[9] in $YBa_2Cu_3O_{7-x}$. Clearly, from Figs. 2a and 3a, the anomalous drop across T_c arises solely from the Cu signal. A similar conclusion can be drawn from the $(Bi_{1.7}Pb_{.3})Sr_2Ca_1Cu_2O_x$ measurements in Fig. 3b, where the data from the individual Bi-Pb, Bi-Pb-Sr, and Bi-Pb-Sr-Cu gates are plotted separately (solid circles, open circles, and solid squares, respectively). Because of the larger number of channels in the Bi-Pb-Sr-Cu gate, these data represent a greater number of total counts, and therefore exhibit less statistical scatter than the data from the other two gates. The total increase in the FWHM between 295 and 35K is only 0.08-0.1° for the Bi-Pb, the Bi-Pb-Sr, and the Bi-Pb-Sr-Cu gates. However, the latter results do show a significant increase across T_c, while the former two data sets show no clear change between 100 and 60K. The anomaly at T_c in $(Bi_{1.7}Pb_{.3})Sr_2Ca_1Cu_2O_x$ has been confirmed using Cu Kα x-ray measurements.[12] Thus, as was the case for $ErBa_2Cu_3O_{7-x}$, the abrupt increase in the FWHM across T_c is found only in the gate containing the Cu signal.

The FWHM results shown in Fig. 3 were analyzed by the method described by Gemmel[8] for ion-channeling in polyatomic crystals. In this approach, the effects of the [001] oxygen rows on channeling are ignored because of their very weak continuum potential, and weighted-average atomic numbers and interatomic distances are assumed for the strong rows. Two strong rows are present along [001] in $ErBa_2Cu_3O_{7-x}$; one contains only Cu and O atoms, the other only Er and Ba. Only one strong [001] row is present in $(Bi_{1.7}Pb_{.3})Sr_2Ca_1Cu_2O_x$, and it contains all five (Pb, Bi, Sr, Cu and O) elements. The continuum approach[19] was then employed, taking into account the improvements obtained from the computer simulation studies of Barrett,[20] to obtain u_1, the average atom root-mean-square atomic displacement (static plus thermal) perpendicular to the channeling ([001]) direction.

For $(Bi_{1.7}Pb_{0.3})Sr_2Ca_1Cu_2O_x$, this analysis showed that the incommensurate phase modulation found previously in this material has a pronounced effect on the ion channeling behavior. For example, Gao et al.[13] report sinusoidally varying static displacements in $Bi_2Sr_2Ca_1Cu_2O_x$ of up to 0.04 nm for the Bi and Sr atoms in the a- and c-directions, and up to 0.03 nm for the Cu atoms in the c-direction only. The net atomic displacements will of course be somewhat larger (~0.01 nm) due to thermal vibrations. Ikeda et al.[14] have observed related effects in Pb-doped specimens such as employed here. [001] axial scans are essentially insensitive to atom displacements in the c-direction, but are directly affected by the a- and b-axis displacements. It was found[12] that by assuming typical thermal vibration amplitudes of ~0.01 nm, and an average static modulation of ~0.02 nm, the analysis[21] reproduced the observed data very well, i.e. the narrowing of the FWHM by ~50%, the weak dependence of the FWHM on

FIGURE 3
FWHM of axial scans as a function of measurement temperature for (a) $ErBa_2Cu_3O_{7-y}$ (Er-Ba gate, open circles; Er-Ba-Cu gate, solid circles) and (b) for $Bi_{1.7}Pb_{0.3})Sr_2Ca_1Cu_2O_x$.

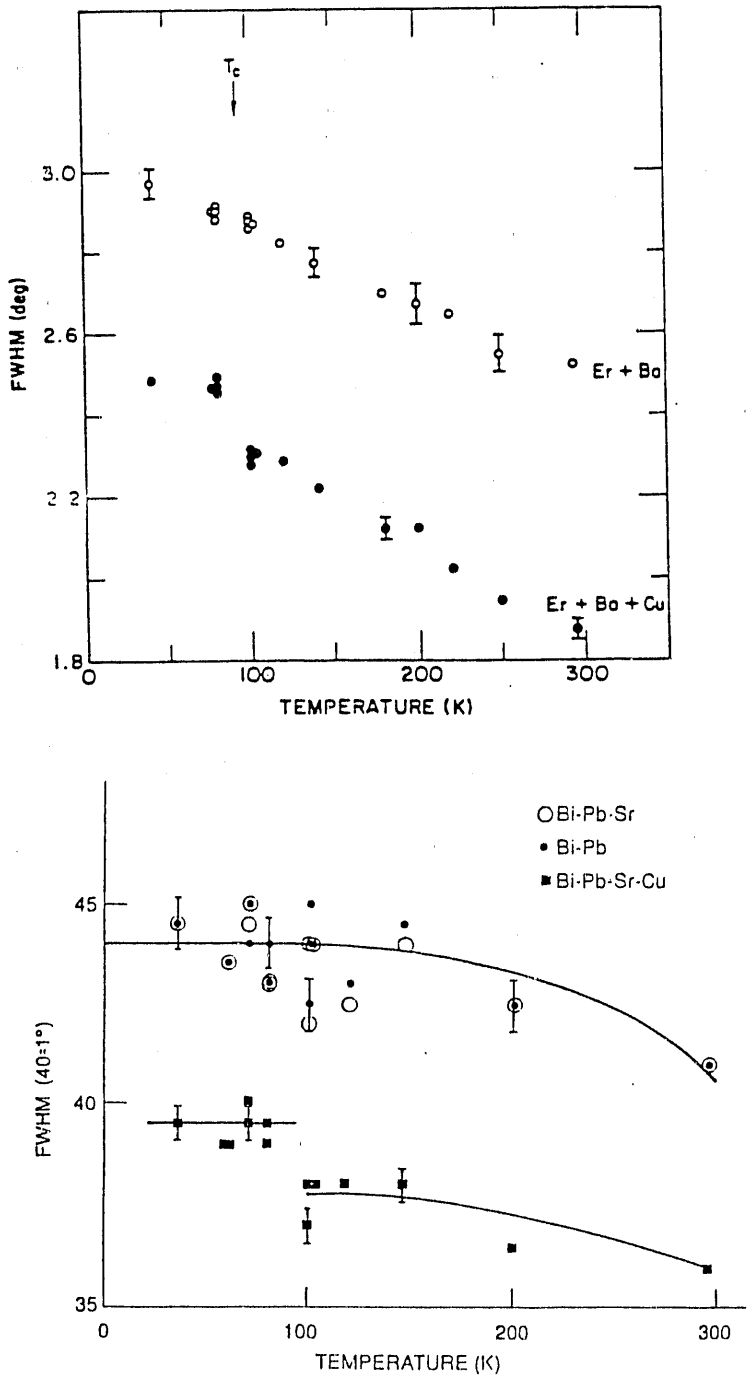

measurement temperature, and the observed minimum yield of 6-10%.

In summary, ion-channeling along the [001] axis in high-quality $(Y/Er)Ba_2Cu_3O_{7-x}$ and $(Bi_{1.7}Pb_{0.3})Sr_2Ca_1Cu_2O_x$ single crystals reveals the following: (1) an anomaly is observed across the superconducting transition in displacements (static plus thermal) perpendicular to the c-axis of the Cu atoms; (2) no anomaly is seen in displacements of the (Y/Er)-Ba or Bi-Pb-Sr-Ca atoms; (3) the incommensurate phase modulation, with atomic displacements < 0.04nm, has a very marked effect on the minimum yield, and on the critical angle for channeling and its temperature dependence.

3. ION CHANNELING ALONG [301] AND [331] IN $YBa_2Cu_3O_{7-x}$

In order to characterize the magnitude and direction of the observed anomaly more completely, we have recently extended our channeling measurements in $YBa_2Cu_3O_{7-x}$ to directions off the c-axis. Additional motivation for examining directions off the c-axis was provided by the recent pulsed neutron diffraction study in $Tl_2Sr_2Cu_2Ca_1O_x$ by Toby et al.[22], in which measurements of the atomic pair distribution functions were interpreted to show large (~.03 nm) anomalous displacements of the Cu and O atoms along the c-axis at T_c. Unfortunately, none of the crystals available to us are sufficiently thick to permit channeling measurements directly along the a- or b-directions. As a compromise, the [301] and [331] directions were selected. These two major directions contain strong atomic rows for channeling, and provide information on c-axis displacements.

Because the well known twins in $YBa_2Cu_3O_{7-x}$ involve simply a switching of the a and b crystal directions, there is no effect of the twins on ion channeling along [001]. However, twinning

becomes a major complication along other directions. For example, both equivalent [301] directions produced very poor channeling scans ($\chi_{min} > 70\%$) because of this twinning. We note however, that areas can be found on the single crystal specimens in which the twinning occurs only along one of the two otherwise equivalent (110) planes. This means that along one of the [331] directions there will be no effect from the twinning, while along the other [331] direction there should be two channeling dips separated by an angle Ø where

$$Ø/2 = 90 - 2\tan^{-1}[a/b]; \quad Ø = 1.88°.$$

Axial scans taken along the two different [331] directions with 1.5 MeV ^{4}He, and a gate which accepts RBS counts from just Y and Ba, are shown in Fig. 4 a and b. Indeed, in Fig. 4a we see the 1.88° splitting of the dips induced by twinning, and the resultant poor minimum yields. It is also evident from this figure that due to this splitting, it is no longer possible to determine accurately any changes in the FWHM occurring between 100 and 40K, i.e. above and below T_c.

However, as expected, reasonably good channeling is observed along the other [331] direction (Fig. 4b), with a minimum yield of ~10% even for the Y-Ba-Cu gate. The 10% minimum yield is readily accounted for by noting that the atomic rows along the [331] direction contain atoms displaced by ~0.02 nm from the geometric center of the row. The three scans shown in Fig. 4b taken first at 80, then 100, then finally 70 K, reveal a clearly reproducible increase in the FWHM of 6% across T_c. Note that this increase (0.09° in the FWHM) represents the square root of the sum of the squares of the contributions from the changes in displacements both perpendicular and parallel to the c-axis. Since this increase is similar to that seen above for displacements perpendicular to the c-axis, it is clear that the parallel displacements cannot be any larger. Hence, the interpretation of the pair distribution results given by Toby et al.[22] is clearly not applicable to $YBa_2Cu_3O_{7-x}$.

Although it was not possible to obtain good axial scans along any of the [301] directions as discussed above in twinned crystals, we were able to obtain quite respectable minimum yields in detwinned crystals. Two examples of [301] RBS scans from a detwinned crystal are shown in Fig. 5. The upper scan was taken at a temperature of 100 K; the lower at 80 K. The minimum yield of $\lesssim$20% in this case is due partly to the existing atomic displacements on the order of 0.02 nm perpendicular to the row, and possibly also to the presence of some remaining twins. Again, the fact that the increase in the FWHM across T_c is very similar to that observed in the [001] direction indicates that the displacements parallel to the c-direction cannot be substantially larger than the ~0.015 nm found for the perpendicular displacements.

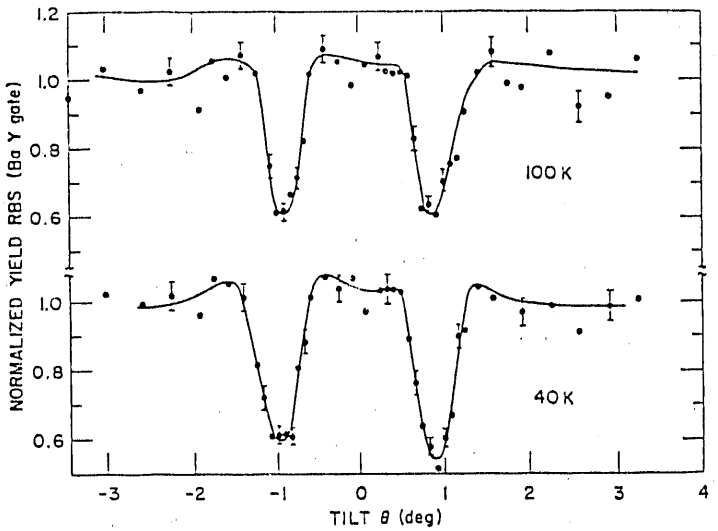

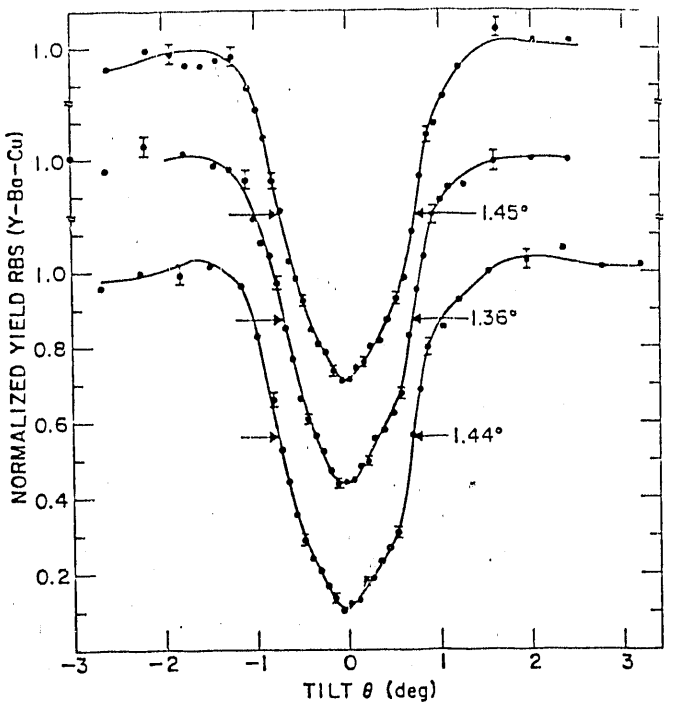

FIGURE 4
[331] axial scans taken with 1.5 MeV He in a twinned $YBa_2Cu_3O_{z-x}$ crystal. The unidirectional twinning splits the axial dips in (above; Y-Ba gate) by 1.88°, but does not affect scans taken at 90° to this axis (above right; Y-Ba-Cu gate; 80, 100 and 70 K).

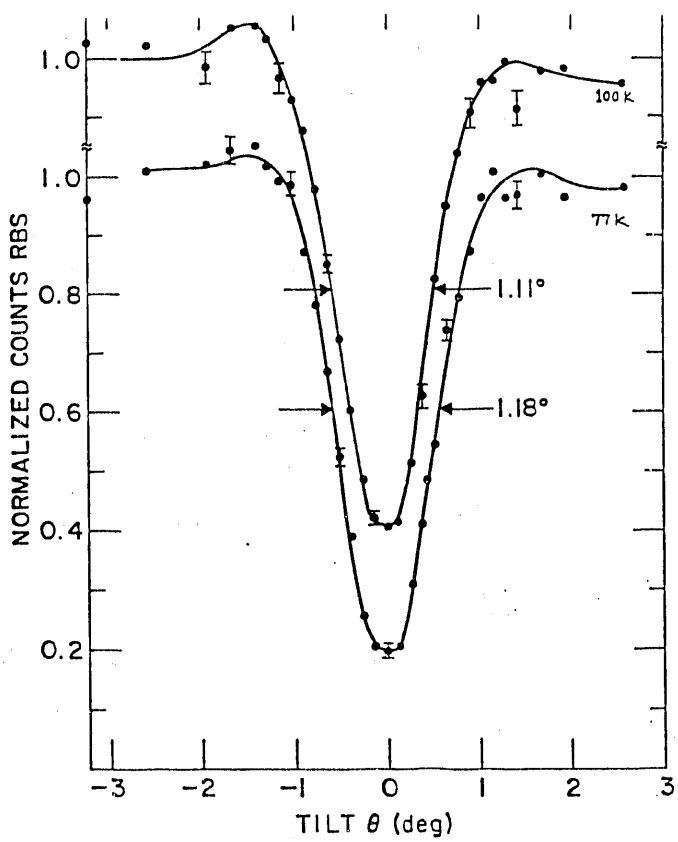

FIGURE 5
RBS axial scans taken with 1.5 MeV He along a [301] direction in a detwinned $YBa_2Cu_3O_{z-x}$ crystal at temperatures of 100 (upper curve) and 77 (lower curve) K.

REFERENCES

1. M. Francois, A. Junod, K. Yvon, A. W. Hewat, J. J. Capponi, P. Strobel, M. Marezio, and P. Fischer, Solid State Commun. 66, 1117 (1988).

2. R. P. Sharma, F. J. Rotella, J. D. Jorgensen, and L. E. Rehn (unpublished).

3. P. M. Horn, D. T. Keane, G. A. Held, J. L. Jordan-Sweet, D. L. Kaiser, F. Holtzberg, and T. M. Rice, Phys. Rev. Lett. 59, 2772 (1987).

4. D. J. Bishop, A. P. Ramirez, P. L. Gammel, B. Batlogg, E. A. Rietman, R. J. Cava, and A. J. Millis, Phys. Rev. B 36, 2408 (1987).

5. A. Migliori, Ting Chen, A. Alavi, and G. Grüner, Solid State Commun. 63, 827 (1987).

6. R. M. Macfarlane, H. J. Rosen, E. M. Enger, R. D. Jacowitz, and V. Y. Lee, Phys. Rev. B 38, 284 (1988).

7. S. L. Cooper, M. V. Klein, B. G. Pazol, J. P. Rice, and D. M. Ginsberg, Phys. Rev. B 37, 5920 (1988).

8. T. Ruf, C. Thomsen, R. Liu, and M. Cardona, Phys. Rev. B 38, 11985 (1988).

9. R. P. Sharma, L. E. Rehn, P. M. Baldo, and J. Z. Liu, Phys. Rev. B 38, 9287 (1988).

10. R. P. Sharma, L. E. Rehn, P. M. Baldo, and J. Z. Liu, Phys. Rev. Lett. 62, 2869 (1989).

11. R. P. Sharma, L. E. Rehn, P. M. Baldo, and J. Z. Liu, Phys. Rev. B 40, 11396 (1989).

12. L. E. Rehn, R. P. Sharma, P. M. Baldo, Y. C. Chang and P. Z. Jiang, Phys. Rev. B, in press, (1990).

13. Y. Gao, P. Lee, P. Coppens, M. A. Subramanian, and A. W. Sleight, Science 241, 954 (1988).

14. Y. Ikeda, M. Takano, Z. Hiroi, K. Oka, H. Kitaguchi, J. Takada, Y. Miura, Y. Takedo, O. Yamamoto, and H. Mazaki, Jpn. J. Appl. Phys. 27, L2067 (1988).

15. See, e.g., L. C. Feldman, J. W. Mayer, and S. T. Picraux, Materials Analysis by Ion Channeling (Academic, New York, 1982).

16. Donglu Shi, Ming Tang, Y. C. Chang, P. Z. Jiang, K. Vandervoort, B. Malecki and D. J. Lam, Appl. Phys. Lett. 54(23), 2358 (1989).

17. T. Kobayashi, S. Takekawa, K. Shigematsu, T. Takahashi, M. Iwaki, H. Sakairi, H. Takahara and M. Aono, Nucl. Instrum. and Meth. B45, 480 (1990).

18. D. S. Gemmell, Rev. Mod. Phys. 46, 129 (1974).

19. J. Lindhard, K. Dan. Vidensk. Selsk. Mat. Fys. Medd. 34, No. 14 (1965).

20. J. H. Barrett, Phys. Rev. B 3, 1527 (1971).

21. W.-K. Chu, J. W. Mayer and M.-A. Nicolet, Backscattering Spectrometry (Academic Press, New York, 1978).

22. B. H. Toby, T. Egami, J. D. Jorgensen and M. A. Subramanian, Phys. Rev. Lett. 64, 2414 (1990).

END

DATE FILMED

12/19/90